



ELSEVIER

Analytica Chimica Acta 395 (1999) 119–132

ANALYTICA  
CHIMICA  
ACTA

## Evaluation of a seawater equilibrator for shipboard analysis of dissolved oceanic trace gases

James E. Johnson<sup>a,b,\*</sup>

<sup>a</sup>Joint Institute for the Study of the Atmosphere and Ocean, University of Washington, Seattle, WA 85115, USA

<sup>b</sup>NOAA, Pacific Marine Environmental Laboratory, 7600 Sand Pt. Wy. NE, Seattle, WA 98115, USA

Received 25 November 1998; received in revised form 1 April 1999; accepted 16 April 1999

### Abstract

Equilibrators have been used for years to obtain gas phase samples for measurement of the partial pressure of dissolved trace gases in near surface seawater. For air–sea exchange studies these measurements assume (1) complete and instantaneous equilibration and (2) that the water sampled is representative of the water in contact with the atmosphere. We present a simple mathematical model to evaluate the factors that determine the equilibration time constant for any gas of known solubility and to determine the deviation from equilibrium that arises from any vent flow of air into the equilibrator headspace. Both these expressions are functionally dependent on a dimensionless equilibrator coefficient  $\varepsilon$ . The model predictions were tested using measurements under field conditions utilizing two gases of widely differing solubility, carbon dioxide and carbon monoxide. For both these gases we show that the value of  $\varepsilon$  for our particular equilibrator is about 0.3–0.4. We also present a depth profile of CO in the top 5 m of the open ocean which demonstrates that seawater sampled through a ship's water inlet at 5 m depth is representative of surface water. © 1999 Elsevier Science B.V. All rights reserved.

*Keywords:* Equilibrator; Trace gases

### 1. Introduction

The ocean is a major source or sink of many atmospheric trace gases that are believed to influence climate. Assessing the air–sea exchange of a gas requires measurements of the partial pressure of the gas in the surface ocean water and the overlying atmosphere. Most instrumentation for trace gas analysis (GC, NDIR) requires samples to be in the gas phase, not the liquid phase. On research ships, where relatively large flows of near surface sample water are

available, equilibrators are commonly used to convert a liquid phase sample to a gas phase sample. In an equilibrator a gas phase headspace is held fixed while the liquid phase is continuously replaced by a sample water stream that showers through the headspace. Equilibrators have been used for oceanic measurements of CO<sub>2</sub>, N<sub>2</sub>O, CH<sub>3</sub>CCl<sub>3</sub>, CO, CH<sub>4</sub>, DMS and other gases [1–7]. In these equilibrators it is assumed that the headspace air will come to full equilibrium so that the partial pressure of the trace gas in the headspace ( $p_e$ ) will equal the partial pressure of the gas in the sample water stream ( $p_w$ ) as:

$$p_w = p_e \quad (1)$$

\*Fax: +1-206-526-6744; e-mail: johnson@pmel.noaa.gov

Assuming an ideal gas, this is equivalent to saying that the trace gas concentration ( $C_e$ ) in the headspace is in equilibrium with the trace gas concentration in the sample water stream ( $C_w$ ) so that

$$C_w = \alpha C_e \quad (2)$$

where  $C_e$  and  $C_w$  are in units of moles per unit volume, and  $\alpha$  is the Ostwald solubility coefficient, defined as the gas phase volume, at standard pressure and temperature  $T$ , contained in a unit volume of water at temperature  $T$  when the partial pressure of the gas in solution is 1 atm [8]. Since  $\alpha$  is a function of temperature and salinity, the temperature in the equilibrator and the salinity of the sample water must be known in order to calculate  $C_w$  from the measured  $C_e$ . Likewise, measurements must be made of any difference in temperature between the equilibrator headspace and the ambient water so that the partial pressure of the gas in the ambient water can be calculated from the partial pressure of the gas in the equilibrator using the temperature dependence of the gas solubility.

Most users of equilibrators have assumed instantaneous equilibrium and have used Eq. (1) or Eq. (2) to determine the amount of dissolved trace gas in their inlet sample water from their measured headspace concentrations. However, equilibration is not an instantaneous process and there is a delay between any change in  $C_w$  in the sample inlet and the corresponding change of  $C_e$  in the equilibrator headspace. This delay can range from minutes to hours depending on the design of the equilibrator, the sample flow rates and the solubility of the trace gas in question.

The headspace concentration also can deviate from equilibrium if there is air exchange between the headspace and the local atmosphere. If this is the case, it can be shown that the headspace can never reach perfect equilibrium but must deviate from perfect equilibrium by some amount. Most equilibrators are vented to the local atmosphere to maintain constant pressure and volume in the headspace and thus allow a small gas flow between the headspace and the local atmosphere. Therefore, most working equilibrators do not reach perfect equilibrium. The deviation from true equilibrium may or may not be significant [2,9].

The primary purpose of this work is to determine and quantify the factors that control the equilibration time constant and deviations from equilibrium of a

working equilibrator. Instead of using Eq. (1) or Eq. (2) with the assumption of instantaneous and complete equilibration, we have constructed two simple mathematical models to examine the response of a working equilibrator to any particular trace gas of known solubility. These simple models were tested during field conditions in experiments that are described in Section 2 of this work. Although these models describe this particular equilibrator, the results we derive should be applicable to equilibrators based on the same principles but different design parameters.

A second purpose of this work is to investigate whether seawater sampled from a ship's underway seawater intake is representative of the water near the air–sea interface. Using CO as a tracer of near surface trace gas concentrations we show that CO concentrations a few cm below the surface are equivalent to those in water collected at a depth of 5 m, a typical depth for underway sample water inlets on research ships.

## 2. Experimental methods

The particular equilibrator used in this study has been used by our group to make numerous measurements over the past 8 years. It is based on the design of Ray Weiss (Scripps Institution of Oceanography) and in this paper will be called the 'Weiss equilibrator'. The Weiss equilibrator (Fig. 1) is made of acrylic and in normal operation has a sample water stream of 13–20 l min<sup>-1</sup> and a headspace volume of 19 l. It was designed for use with the soluble gases CO<sub>2</sub> and N<sub>2</sub>O. The essential features of the Weiss equilibrator are that sample water is forced through small holes in a plate at the top of the headspace with a minimal head pressure of 0.2 atm, and then dribbles through the main body of the headspace. The lower half of the main chamber serves as an air lock so that the sample water may freely move through the equilibrator, but the headspace air is trapped within the equilibrator. Air is drawn continuously from the equilibrator headspace from a tube connected with an air pump, and almost all this air is returned to the equilibrator. Typically, occasional aliquots of sample are allowed to pass into a gas analysis system. This equilibrator is technically a two-stage equilibrator, as there is a central chamber to which the return air from the air pump and air from the

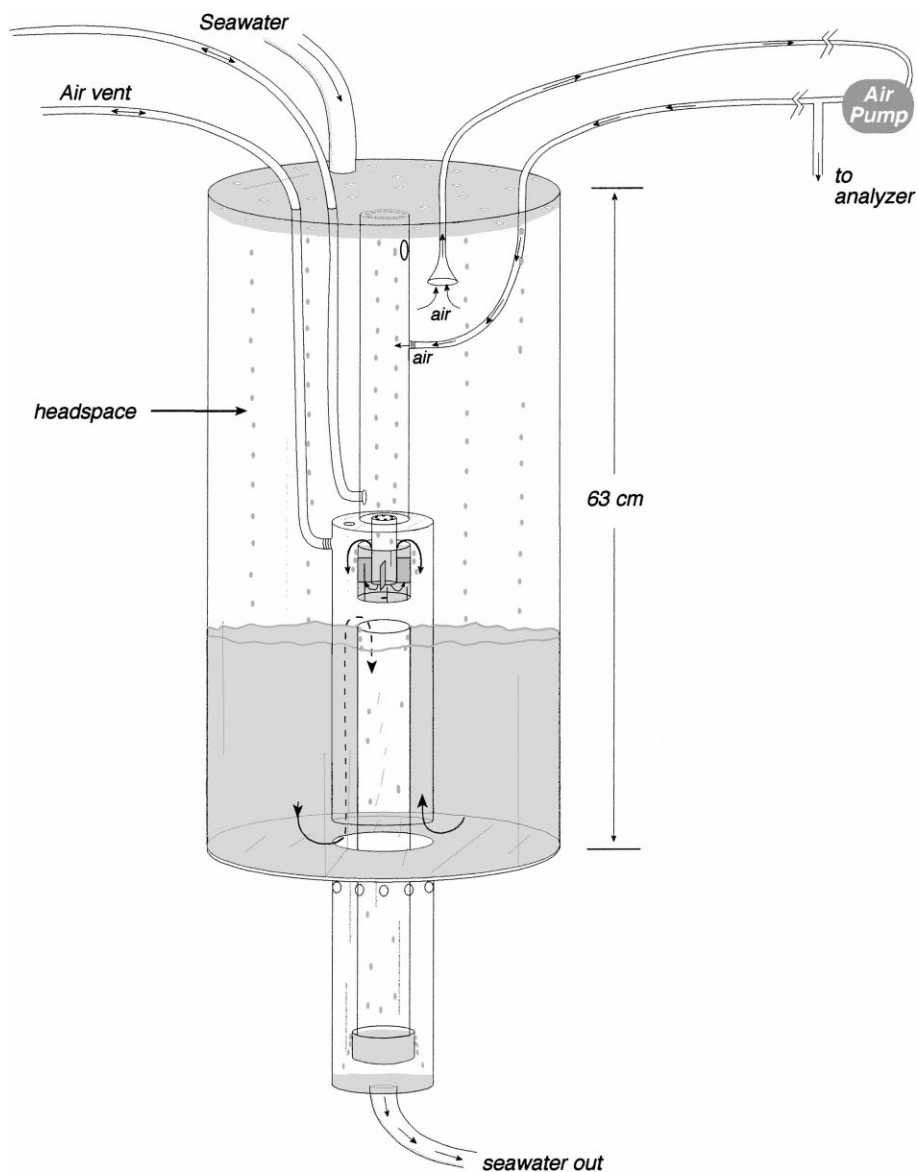


Fig. 1. A schematic representation of the Weiss equilibrator.

vent tube enters. However, because the residence time for air in the central chamber is typically much less than a minute, in the models described below the simplifying mathematical assumption will be made that the equilibrator headspace is a single stage, and that it is well mixed.

CO<sub>2</sub> was determined using a nondispersive infrared (NDIR, LiCor, model 6252) analyzer [2]. The NDIR analyzer produced a continuous analogue signal that

was digitized and stored as 1 min averages. The system was designed to sample three gas standards during the first 30 min of each hour, ambient air from the bow sampling line for the next 10 min and air from the equilibrator headspace for the last 20 min of each hour.

CO was determined with a gas chromatograph (GC) with a reduction gas detector [6]. The CO system used discrete injections every 5 min, but was on a 35 min

cycle such that two of the seven injections within the interval were equilibrator headspace air, the rest were air samples or standards.

### 3. Models

#### 3.1. Level one model

We first assume that the trace gas in question is not created or destroyed by chemical or biological reactions inside the equilibrator and that surfaces inside the equilibrator neither absorb nor emit the trace gas. The simplest model, the level one model, further assumes that the headspace is sealed from the outside atmosphere and no exchange or venting occurs between the equilibrator and the surrounding atmosphere. This assumption greatly simplifies the mathematical model. The effect of venting will be examined in the level two model.

In order to introduce time-dependent terms into an equilibrator model the flux of a gas between the headspace and the sample water stream must be parameterized. In the level one model this flux is

$$V_e \frac{dC_e}{dt} = Q_w(C_w - C_{w0}) \quad (3)$$

where  $V_e$  is the volume of the headspace,  $C_e$  is the mass concentration of the trace gas in the headspace,  $Q_w$  is the volumetric flow rate of the sample water stream through the equilibrator,  $C_w$  is the concentration of the trace gas in the sample water stream as it enters the equilibrator and  $C_{w0}$  is the concentration of the trace gas in the sample water stream as it leaves the equilibrator. (All concentrations are in units of mass per unit volume). Eq. (3) is the mass continuity equation for the equilibrator headspace and states that the gain (or loss) of trace gas in the headspace must be exactly matched by the loss (or gain) of trace gas to (from) the sample water stream. The left hand side of Eq. (3) is the time rate of change of mass of the trace gas in the equilibrator headspace. The right hand side of Eq. (3) is the rate at which the trace gas leaves the sample water stream and enters the headspace.

If the sample water stream fully equilibrates with the headspace as it falls through it, then  $C_{w0}$  will be in equilibrium with  $C_e$  and  $C_{w0}$  will be a function of  $C_e$  as

in Eq. (2), and Eq. (3) can be expressed as

$$V_e \frac{dC_e}{dt} = Q_w(C_w - \alpha C_e) \quad (4)$$

The right hand side of Eq. (4) represents the maximum amount of trace gas that is thermodynamically possible to flux out of the sample water stream. However, because the transfer between the liquid and gas phases is a kinetic process it is unrealistic to assume that the maximum possible amount will transfer. It is more realistic to assume that for any given sample water stream flow a dimensionless equilibrator coefficient,  $\varepsilon$ , will be a constant and independent of the existing disequilibrium ratio,  $C_w/(\alpha C_e)$ . This  $\varepsilon$  is a number between 0 and 1 and will be 1 if the sample water stream is fully equilibrated with the headspace when it leaves contact with the headspace.  $\varepsilon$  is simply the fraction of the potentially available trace gas that transfers into or out of the sample water stream, when it is in contact with the headspace. The fact that  $\varepsilon$  is not equal to 1 does not mean that the equilibrator headspace does not come to full equilibrium, it only means that it takes longer to reach full equilibrium. Utilizing this equilibrator coefficient, Eq. (4) becomes:

$$V_e \frac{dC_e}{dt} = \varepsilon Q_w(C_w - \alpha C_e) \quad (5)$$

If we define  $\tau_1$  as

$$\tau_1 = \frac{V_e}{Q_w \varepsilon \alpha} \quad (6)$$

then a time-dependent solution of Eq. (5), for  $C_e$  assuming an initial  $C_e$  of  $C_i$  that is not in equilibrium with  $C_w$  is

$$C_{e(t)} = \left( C_i - \frac{C_w}{\alpha} \right) e^{-\left( \frac{t}{\tau_1} \right)} + \frac{C_w}{\alpha} \quad (7)$$

The solution Eq. (6) shows that for any step change in  $C_w$ ,  $C_e$  will exponentially relax to the steady state concentration  $C_w/\alpha$  with a time constant  $\tau_1$ , the time constant of the level one model.  $\tau_1$  is a primary parameter that can be used to evaluate the performance of the equilibrator. If it is short, then the usual assumption of quick and complete equilibration is likely justified. However, to know  $\tau_1$ , the equilibrator coefficient  $\varepsilon$ , must first be known. Although it may be possible to predict theoretically, one would have to

model the kinetic transfer of trace gases from water droplets as they fall through the equilibrator headspace. Such a model is beyond the scope of this paper. The second half of this paper will provide experimental evidence that under normal operating conditions the value of  $\varepsilon$  is about 0.3–0.4 for several trace gases in this particular equilibrator.

In the case of  $\text{CO}_2$ , chemical enhancement may increase the gas flux from the sample water stream to the headspace. The enhanced flux would arise due to replacement of dissolved  $\text{CO}_2$  by reaction of dissolved  $\text{HCO}_3^-$  with  $\text{H}_2\text{O}$  or  $\text{H}^+$ . In effect, there would be an extra term on the right hand side of Eq. (3). However, using ambient oceanic carbon species concentrations and kinetic rate constants [10], it can be shown that the time constant for replacement of dissolved  $\text{CO}_2$  by this reaction is of order 10–100 s for ambient oceanic temperatures and pH, which is much longer than the time the sample water appears to be in contact with the headspace. Thus, for  $\text{CO}_2$  this process may enhance the flux in the equilibrator by only a small amount and it is not a significant factor in the determination of  $\tau_1$ .

### 3.2. Level two model

Given enough time ( $3\text{--}5 \tau_1$ ), according to Eq. (7),  $C_e$  will reach its steady state value  $C_{e(ss)}$  which in the level one model is perfect equilibrium because Eq. (5) contains no sources or sinks of the trace gas to the headspace other than flux from the sample water. However, under realistic field conditions the equilibrator ‘vents’, that is air is removed from the headspace and must be replaced by ambient air from the vent tube. Venting can arise from at least three causes. First, for most analytical systems, headspace air is removed for sample analyses. Second, the sample water stream may not be in equilibrium with the major species in air, nitrogen and oxygen. If the sample water stream is over or under saturated, the major species will be added or removed from the headspace by the sample water stream. Third, although there is an airlock to prevent headspace air from leaving with the sample stream, small bubbles may form and be carried through the air lock. Of the three effects we believe the last one is the most serious in our equilibrator and we have measured typical venting rates of ambient air into the equilibrator head-

space of  $0.02\text{--}0.04 \text{ l min}^{-1}$  when no sample gas is being removed for analysis.

The level two model includes the effects of venting by amending Eq. (5) to include vent terms

$$V_e \frac{dC_e}{dt} = Q_w \varepsilon (C_w - \alpha C_e) + Q_v (C_a - C_e) \quad (8)$$

where  $Q_v$  is the volumetric vent flow of ambient air into the equilibrator (positive in, negative out) and  $C_a$  the concentration of the trace gas in the ambient atmosphere. The last term in Eq. (8) is the time rate at which the equilibrator headspace gains trace gas from the ambient atmosphere (or the rate the headspace loses trace gas if negative).

If we define a venting time constant  $\tau_v$  as

$$\tau_v = \frac{V_e}{Q_v}$$

and further define  $\tau_2$  as

$$\frac{1}{\tau_2} = \frac{1}{\tau_1} + \frac{1}{\tau_v} \quad (9)$$

then the time-dependent solution of Eq. (8), for  $C_e$  assuming an initial  $C_e$  of  $C_i$  that is not in equilibrium with  $C_w$  is

$$C_{e(t)} = \frac{(C_w/\alpha\tau_1)(1 - e^{-t/\tau_2}) + (C_a/\tau_v)(1 - e^{-t/\tau_2}) - (C_i/\tau_2)e^{-t/\tau_2}}{1/\tau_2} \quad (10)$$

Thus the equilibrator headspace gas concentration will exponentially relax with a time constant of  $\tau_2$  to a new steady-state concentration as  $t \rightarrow \infty$  of

$$C_{e(ss)} \rightarrow \frac{(C_w/\tau_1\alpha) + (C_a/\tau_v)}{(1/\tau_1) + (1/\tau_v)} = \frac{Q_w \varepsilon C_w + Q_v C_a}{Q_w \varepsilon \alpha + Q_v} \quad (11)$$

If  $Q_v$  goes to zero then  $C_{e(ss)}$  reduces to  $C_w/\alpha$ , i.e., the level one model with no vent terms. If  $Q_v$  is non-zero then  $C_{e(ss)}$  is not equal to  $C_w/\alpha$  and the headspace does not fully equilibrate. A measure of the incompleteness of equilibration is the equilibration ratio,  $\Delta$ , which can be defined as

$$\Delta = \frac{C_{e(ss)}}{(C_w/\alpha)} \quad (12)$$

For perfect equilibration,  $\Delta$  will be equal to unity. Since  $\Delta$  differs from 1 by only a small value if the

equilibrator is functioning correctly a more useful parameter, the disequilibrium factor,  $D$ , can be defined as

$$D = 1 - \Delta \quad (13)$$

where  $D$  will be zero for perfect equilibration and will be either greater or less than zero during disequilibrium.

From Eqs. (11) and (13) it can be shown that the equilibration ratio,  $\Delta$ , at steady state is:

$$\Delta = \frac{C_{e(ss)}}{(C_w/\alpha)} = \frac{Q_w \varepsilon \alpha + (\alpha Q_v C_a / C_w)}{Q_w \varepsilon \alpha + Q_v} \quad (14)$$

and  $D$ , the disequilibrium is

$$D = 1 - \Delta = \frac{(Q_v/Q_w)(1 - (C_a \alpha / C_w))}{\varepsilon \alpha + (Q_v/Q_w)} \quad (15)$$

For all but the highest  $Q_v$  coupled with the lowest  $\alpha$ ,  $Q_v/Q_w \ll \varepsilon \alpha$ , and Eq. (15) simplifies to

$$D = \frac{Q_v}{Q_w} \left( \frac{1}{\varepsilon \alpha} \right) \left( 1 - \frac{C_a \alpha}{C_w} \right) \quad (16)$$

This last relationship shows that  $D$  is the product of three factors. The first factor, the ratio of the vent flow to the water flow shows that  $D$  is linearly dependent on  $Q_v$ . The second factor shows that  $D$  scales inversely with  $\varepsilon \alpha$  the product of the equilibrator coefficient and the solubility, thus  $D$  will be less for more soluble gases. The last factor shows that  $D$  also depends on the existing disequilibrium between the sample water and the local ambient atmosphere.

These models make some predictions. First, they predict that the concentration of a trace gas in the equilibrator headspace will follow a step change in the concentration of that gas in the sample inlet stream with an exponential relaxation to the new concentration. Further, the exponential time constant can be determined from measured values of the headspace volume, the water flow rate, the solubility of the trace gas, and the equilibrator coefficient  $\varepsilon$ . Unfortunately, the equilibrator coefficient,  $\varepsilon$ , cannot be determined easily from theory. However, these equilibrator models can be verified and  $\varepsilon$  determined by observing the response of a trace gas concentration in the equilibrator headspace to a step change in concentration of either the incoming gas stream or the headspace itself. This test can first determine if the response of the trace gas concentration is an exponential function as pre-

dicted by Eq. (10). If the response appears to be exponential then the time constant can be obtained by a mathematical fit. Once the time constant is obtained, then if the solubility, water flow rate and equilibrator volume are known, Eq. (6) can be used to determine  $\varepsilon$ , the equilibrator coefficient. Alternatively, the equilibrator can be put into disequilibrium by introducing a large (but measured) vent flow. Then all the factors in Eq. (15) except  $\varepsilon$  are known or measured and  $\varepsilon$  can be calculated. These methods were used on recent oceanographic research cruises in experiments using the gases carbon dioxide ( $\text{CO}_2$ ) and carbon monoxide (CO).

## 4. Experimental results

### 4.1. Carbon dioxide experiment

The  $\text{CO}_2$  experiment was performed during the RITS/ACE-1 project in December of 1995, on the NOAA ship DISCOVERER in waters south of Tasmania. The  $\text{CO}_2$  experiment involved two steps. In the first step the equilibrator was thrown into great disequilibrium by pumping approximately 6 l/min of ambient air through the headspace, effectively unsealing it from the ambient air. In the second step the headspace was resealed and the return to equilibrium of  $\text{CO}_2$  in the headspace was observed and the time constant was then determined by fitting the measured response of the equilibrator headspace to an exponential function.

The gas sample lines to each equilibrator during normal operation are shown in Fig. 2(A). In each case one pump (the air pump) continuously drew ambient air through an air sample line from an inlet near the bow of the ship, away from local ship pollution, to the shipboard laboratory. A second pump (the equilibrator pump) drew air from the equilibrator headspace into the laboratory and then returned it to the equilibrator headspace.

Since it was impossible to create a step change in the concentration of  $\text{CO}_2$  in the sample water during the field conditions a step change in the concentration of  $\text{CO}_2$  in the headspace was done instead by replumbing the system as shown in Fig. 2(B). The equilibrator air pump was switched off, and the exhaust line from the air sample pump was sent to the equilibrator. A tee

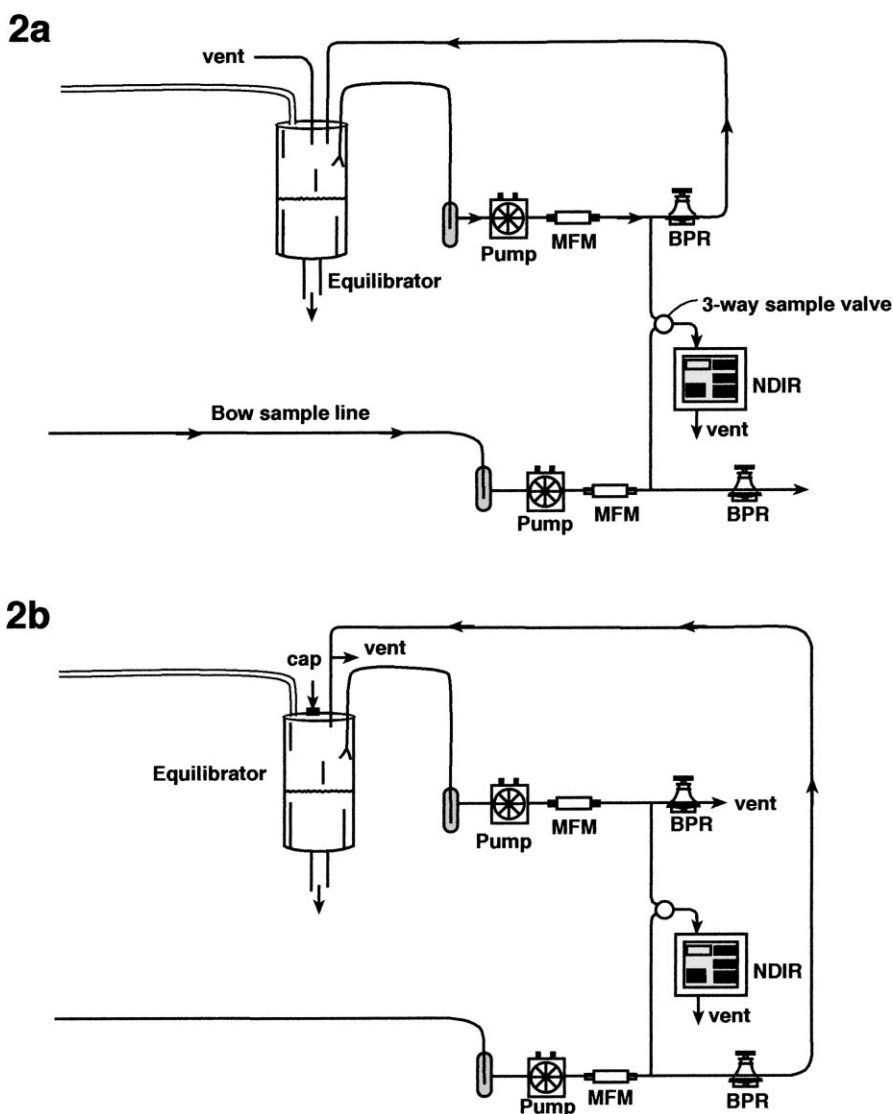


Fig. 2. A schematic representation of the equilibrator flows for the disequilibrium and re-equilibration experiments. MFM and BPR refer to mass flow meter and back pressure regulator, respectively. (A) is the flow setup during normal operating conditions where air is drawn from the equilibrator to a pump located in the ships laboratory, and then is returned back to the equilibrator with only small amounts withdrawn for gas analysis. (B) is the flow setup during the disequilibrium experiment where the air that was withdrawn from the equilibrator was not returned and was replaced in the equilibrator with air that had been collected from the ships air sampling line.

with a vent to the atmosphere was placed near the inlet to the equilibrator return port so that the pressure in the equilibrator remained at atmospheric pressure. Once the plumbing was changed the equilibrator air pump was switched on. The flow leaving each pump was measured with a mass flow meter and the excess flow leaving the vent at the equilibrator return inlet was also

measured, to ensure that air sample flow was greater than the flow of air being drawn into the equilibrator. This caused a massive 'venting flow' of about 6 l/min of ambient air into the equilibrator headspace where trace gas concentrations relaxed to 'steady state', perturbed values. The  $\text{CO}_2$  concentration of the vent air was known because the atmospheric concentration

of CO<sub>2</sub> was measured in the hour immediately before and in the hour immediately after the equilibrator test.

The equilibrator was left in this perturbed condition while the gas analysis system continued its normal hourly cycle. 1 h later, during the next 20 min period at which the headspace gas was being analyzed, the equilibrator air pump was again turned off, the air flow plumbing was returned to its normal state (Fig. 2(A)), and the equilibrator air pump restarted. An example of the output of the CO<sub>2</sub> mixing ratio processed by the NDIR analyzer during the equilibrator test on 4 December is shown in Fig. 3(A). The record first

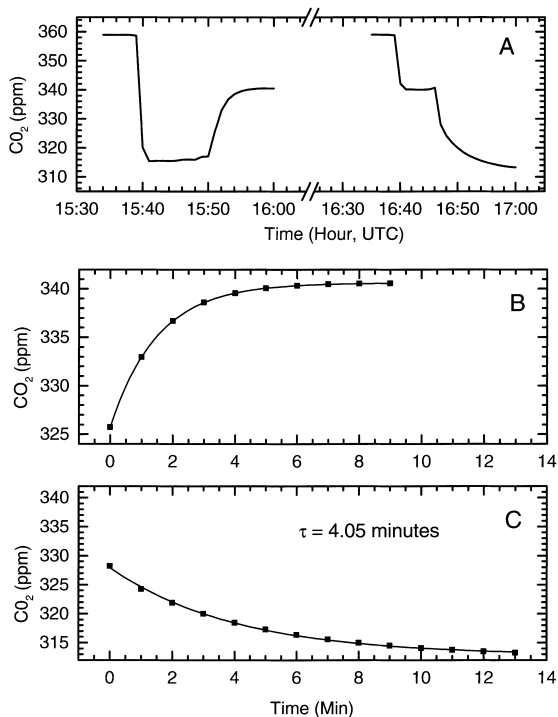


Fig. 3. CO<sub>2</sub> experiment on 4 December. (A) is the concentration of CO<sub>2</sub> as measured by the NDIR instrument showing CO<sub>2</sub> in ambient air (15:30–15:40), the equilibrator headspace in the normal state (15:40–15:47), the transition to the perturbed state (15:47–16:00), air (16:30–16:40), the equilibrator headspace in the perturbed state (16:40–16:48), and the transition back to the normal state (16:48–17:00). (B) is the transition to the perturbed state. The squares are the 1 min data and the line is an exponential function fit to the data, zero time being 15:51. (C) is the transition back to the normal state. Again, the squares are the 1 min data and the line is an exponential function fit to the data, zero time being 16:47. The time constant,  $\tau$ , from the fit to Eq. (17) is given.

shows the atmospheric CO<sub>2</sub> mixing ratio of 360 ppm from 15:30 to 15:40, then the input to the analyzer was automatically switched to sample the equilibrator headspace (with the plumbing in its normal condition, Fig. 2(A)). At 15:47 the plumbing was manually reconfigured to the perturbed condition (Fig. 2(B)) and the CO<sub>2</sub> analyzer recorded the CO<sub>2</sub> in the headspace exponentially relaxing to the perturbed concentration. From 16:00 to 16:30 the CO<sub>2</sub> analyzer sampled three different standards (not shown in Fig. 3(A)). At 16:30 the analysis system repeated the cycle from the previous hour, by measuring air, then the equilibrator headspace, which had been in the perturbed condition from the past hour until 16:46, at which point the equilibrator air flow lines were returned to normal and the headspace concentration exponentially relaxed to its true equilibrium value. Two more equilibrator tests from 5 December and 11 December are shown in Fig. 4(A) and Fig. 5(A), respectively. Table 1 lists the seawater temperature

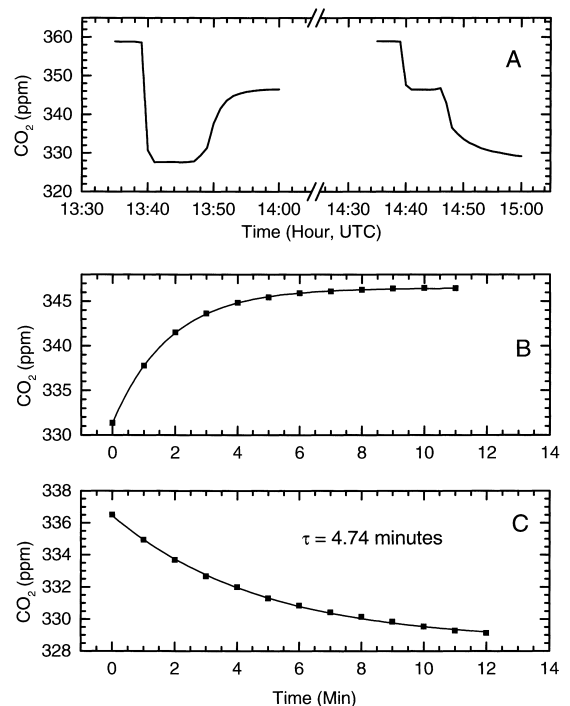


Fig. 4. CO<sub>2</sub> experiment on 5 December. (A), (B) and (C) as in Fig. 3. The zero time for the fit in (B) was 13:49, the zero time for the fit in (C) was 14:48.



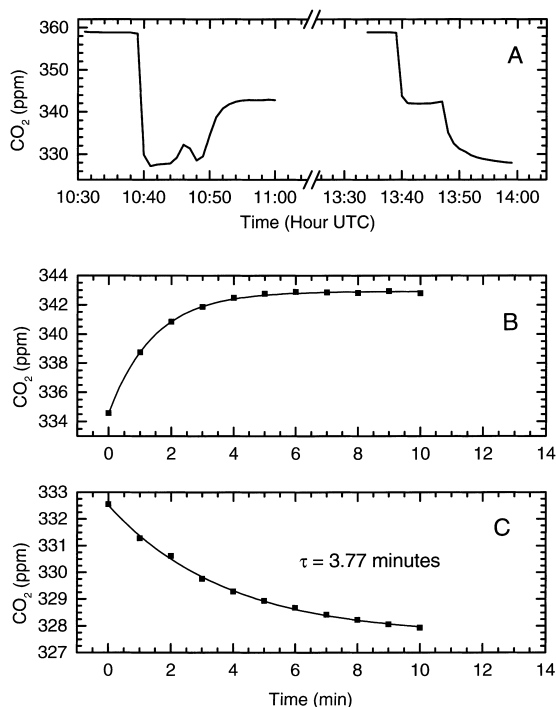


Fig. 5. CO<sub>2</sub> experiment on 11 December. (A), (B) and (C) as in Fig. 3. The zero time for the fit in (B) was 10:50, the zero time for the fit in (C) was 13:49. The bump at 10:46 was due to a delay in the plumbing switch to the perturbed state.

and salinity, the calculated CO<sub>2</sub> solubility and the equilibrator water flow rate for each of the three CO<sub>2</sub> experiments.

#### 4.2. Return to equilibrium test

For each experiment,  $\tau_1$ , was calculated by least-squares fitting the return to equilibrium (the right side of Fig. 3(A), Fig. 4(A) and Fig. 5(A)) to an exponen-

tial of the form:

$$C_e = A + Be^{-t/\tau} \quad (17)$$

where  $A$ ,  $B$ , and  $\tau$  are constants found for each fit. Eq. (17) can be shown to be equivalent to Eq. (7) the time-dependent solution of the level one model to a step change in either  $C_w$  or  $C_e$  (in this case  $C_e$ ). In particular  $A = C_w/\alpha$ , in this experiment the true equilibrium headspace concentration of CO<sub>2</sub> that is in equilibrium with the sample water stream, (in units of ppm),  $B = C_{ei} - (C_w/\alpha)$ , the difference between the headspace CO<sub>2</sub> concentration and the actual perturbed headspace CO<sub>2</sub> concentration at time  $t = 0$ , and  $\tau = \tau_1$ , the fit time constant is the level one time constant. The fits are shown as the solid lines in Fig. 3(C), Fig. 4(C) and Fig. 5(C). The numerical results of the fits are shown in Table 2, where time constants derived from the fits are in the range of 3.8–4.7 min with rms fitting errors in the range of 0.06–0.15 ppm of CO<sub>2</sub>. As can be seen in the plotted fits, (Fig. 3(C), Fig. 4(C) and Fig. 5(C)) and in the small rms errors of the fits it appears that the actual behavior of the equilibrator to a step change in  $C_e$  is indeed an exponential function and Eq. (7) for the level one model does appear to be validated. Using Eq. (6) with these experimentally determined time constants, and the values given for  $\alpha V_e$  and  $Q_w$  from Table 1,  $\varepsilon$  is estimated as 0.32, 0.28, and 0.29.

#### 4.3. Disequilibrium test

Another method to estimate  $\varepsilon$  is to measure the extent of disequilibrium while a large and measured vent flow of ambient air is directed into the equilibrator headspace. This was done during the first half of the re-equilibration tests. Eq. (15) can be

Table 1  
General conditions for the carbon dioxide experiment

|                  | Units | 4 December | 5 December | 11 December |
|------------------|-------|------------|------------|-------------|
| Headspace volume | l     | 19.00      | 19.00      | 19.00       |
| Temperature      | °C    | 12.90      | 13.15      | 11.80       |
| Salinity         | PSU   | 34.90      | 34.85      | 34.67       |
| $Q_w$            | l/min | 15.17      | 14.97      | 17.09       |
| $\alpha$         |       | 0.96       | 0.98       | 1.00        |

$Q_w$  was the measured sample water flow;  $\alpha$  was the CO<sub>2</sub> solubility from [13] converted to dimensionless units of  $\alpha$ .

Table 2  
Carbon dioxide re-equilibration experiment

|                  | Units | 4 December | 5 December | 11 December |
|------------------|-------|------------|------------|-------------|
| <i>A</i> (fit)   | ppm   | 312.80     | 328.58     | 327.62      |
| <i>B</i> (fit)   | ppm   | 15.13      | 7.87       | 4.89        |
| $\tau$ (fit)     | min   | 4.05       | 4.74       | 3.77        |
| rms error of fit | ppm   | 0.15       | 0.06       | 0.06        |
| $\varepsilon$    |       | 0.32       | 0.28       | 0.29        |

*A*, *B* and  $\tau$  were constants calculated from a least squares fit to Eq. (17) of the data shown in Fig. 1(C), Fig. 2(C) and Fig. 3(C);  $\varepsilon$  was calculated from Eq. (6).

rearranged to

$$\varepsilon = \frac{1}{\alpha} \left[ \frac{Q_v}{DQ_w} \left( 1 - \frac{C_a}{C_{et}} \right) - \frac{Q_v}{Q_w} \right] \quad (18)$$

where *D* the disequilibrium can be defined as

$$D = 1 - \frac{C_{ep}}{C_{et}} \quad (19)$$

and *C*<sub>ep</sub> is the CO<sub>2</sub> headspace concentration under a 'steady-state' perturbation during the disequilibrium conditions, and *C*<sub>et</sub> is the CO<sub>2</sub> concentration in the equilibrator headspace when it is at true equilibrium. The true equilibrium concentration, *C*<sub>et</sub>, was measured in the few minutes before the sample plumbing was switched, and the perturbed concentration, *C*<sub>ep</sub>, was measured after the plumbing was switched to its perturbed state. For the disequilibrium experiment all the terms on the right hand side of Eq. (18) were measured except for  $\alpha$ , which can be calculated from

the measured salinity and temperature [11]. Thus,  $\varepsilon$  can be estimated by a method that is independent of the re-equilibration test described above. One small problem is that during the limited time period imposed by the sampling system the equilibrator headspace concentration did not fully relax to its steady-state perturbed value, *C*<sub>ep</sub>. However, assuming that the equilibrator approached its step change in headspace concentration as an exponential relaxation as described by Eq. (10) we can use an exponential fit of the form Eq. (17) to fit the change from an equilibrated headspace to a perturbed headspace (Fig. 3(B), Fig. 4(B) and Fig. 5(B)). In this fit to disequilibrium conditions the fit coefficient *A*, can be used to predict *C*<sub>ep</sub>, and the fit time constant  $\tau$  is  $\tau_2$ , the time constant of the level two model. The results of the fit and the resulting  $\varepsilon$  calculated with Eq. (18) is shown in Table 3 for the three CO<sub>2</sub> experiments with  $\varepsilon$  values of 0.29–0.33, in excellent agreement to the calculated

Table 3  
Carbon dioxide disequilibrium experiment

|                        | Units | 4 December | 5 December | 11 December |
|------------------------|-------|------------|------------|-------------|
| <i>A</i> (fit)         | ppm   | 340.61     | 346.48     | 342.91      |
| <i>B</i> (fit)         | ppm   | −14.88     | −15.12     | −8.36       |
| $\tau$ (fit)           | min   | 1.50       | 1.81       | 1.43        |
| <i>C</i> <sub>a</sub>  | ppm   | 359.19     | 359.03     | 359.10      |
| <i>C</i> <sub>et</sub> | ppm   | 312.80     | 328.58     | 325.82      |
| <i>C</i> <sub>ep</sub> | ppm   | 340.61     | 346.48     | 342.91      |
| <i>Q</i> <sub>v</sub>  | l/min | 6.40       | 6.22       | 6.00        |
| <i>D</i>               |       | −0.09      | −0.05      | −0.05       |
| $\varepsilon$          |       | 0.29       | 0.30       | 0.33        |
| $\tau_2$ predicted     | min   | 1.71       | 1.86       | 1.72        |

*A*, *B* and  $\tau$  were constants calculated from a least squares fit Eq. (17) of the data shown in Fig. 1(B), Fig. 2(B) and Fig. 3(B); *C*<sub>a</sub> and *C*<sub>et</sub> were the means of measured mixing ratio of CO<sub>2</sub> in the atmosphere and in the equilibrator headspace immediately before and after the equilibrator was perturbed for the experiment; *C*<sub>ep</sub> was the 'steady-state' perturbed CO<sub>2</sub> mixing ratio in the headspace (from *A*); *Q*<sub>v</sub> was the measured vent flow of ambient air into the equilibrator during the experiment; *D* was the disequilibrium calculated with Eq. (19);  $\varepsilon$  was the equilibrator coefficient calculated with Eq. (18);  $\tau_2$  was the level two model equilibrator time constant as determined from Eq. (9).

values of re-equilibration experiment which ranged from 0.28 to 0.32.

Another check on the level 2 model is that  $\tau_2$  can be calculated in two different ways. In the first method,  $\tau_2$  is the time constant from the fit to Fig. 3(B), Fig. 4(B) and Fig. 5(B), and second,  $\tau_2$  can be calculated from Eq. (9) using the value of  $\tau_1$  estimated from the re-equilibration experiment, and  $\tau_2$  calculated from the measured values of  $V_e$  and  $Q_v$ . When this is done the mean value of  $\tau_2$  from the fits of 1.58 min compares well to the mean value of 1.76 min calculated using Eq. (9).

#### 4.4. Carbon monoxide experiment

The performance of the equilibrator and the value  $\varepsilon$  was also examined using carbon monoxide (CO). The behavior of CO in the equilibrator has several important differences from that of CO<sub>2</sub>. First the solubility of CO in seawater is about 50 times less than that of CO<sub>2</sub>. Second, where the partial pressure CO<sub>2</sub> in seawater is generally 0.8–1.2 that of atmospheric partial pressure of CO<sub>2</sub>, the partial pressure of CO in surface seawater is almost always a factor of 50–100 times greater than the atmospheric partial pressure. Thus, because of its low solubility the time constant for CO in the equilibrator can be several hours, and because of the low solubility and the large difference between the atmospheric and oceanic CO partial pressures, any venting of ambient air will cause a much greater relative error in headspace CO concentrations than for CO<sub>2</sub>.

The CO test was done using a Weiss equilibrator that was identical to, and located next to, the CO<sub>2</sub> equilibrator on the RITS/ACE-1 project. During normal operation the equilibrator plumbing was similar to Fig. 2(A), the only exception being that a GC system was used in place of the CO<sub>2</sub> NDIR analyzer. As in the CO<sub>2</sub> test the equilibrator plumbing was put into the massive disequilibrium configuration of Fig. 2(B), during which time the CO concentration dropped from the seawater equilibrium value of 2000–4000 ppb to the perturbed value of around 100 ppb. Due to the long time constants for CO, and because of the somewhat irregular sampling schedule we did not wait for steady-state disequilibrium as in the CO<sub>2</sub> case, but rather we determined that the CO concentration was 'low' and then started the re-equilibration.

A problem with the CO experiment that was not present in the CO<sub>2</sub> experiment is that CO has a relatively short lifetime in surface seawater [12,13] and consequently the surface seawater has concentration changes on the time scale of hours, and the spatial variability can be large. To minimize the problem of spatial inhomogeneity the experiments were done while the ship was motionless and holding station. The experiments were also done at night when the surface water CO concentrations were decaying due to biological oxidation, and the photoproduction was not occurring [13]. Due to the nocturnal decay in the CO concentrations the return to equilibrium cannot be treated as easily as was the case for CO<sub>2</sub>, where the surface water concentrations are stable on the time scale of the CO<sub>2</sub> equilibration time constant. To account for the changing surface water concentration we have made the simplifying assumption that during the re-equilibration time, the surface water change was linear in time so that

$$C_w(t) = a + bt \quad (20)$$

Using Eq. (20) and the definition of  $\tau_1$ , Eqs. (5) and (6) can be rearranged to

$$\frac{dC_e}{dt} = \frac{a}{\tau_1} + \frac{\alpha bt}{\tau_1} - \frac{\alpha C_e}{\tau_1} \quad (21)$$

The time-dependent solution of Eq. (21), for  $C_e$  assuming an initial  $C_e$  of  $C_i$  that is not in equilibrium with  $C_w$  is

$$C_e = C_i e^{\frac{-t}{\tau_1}} - \frac{a}{\alpha} (e^{\frac{-t}{\tau_1}} - 1) + \frac{b\tau_1}{\alpha} (e^{\frac{-t}{\tau_1}} - 1) + \frac{bt}{\alpha} \quad (22)$$

Two re-equilibration experiments (Fig. 6) occurred on the nights of 6 December and 8 December. For each experiment the zero time was chosen as the time of the first sample analysis after the re-equilibration had started. The data plotted between  $-5$  and  $-1$  h were the normal CO values in the equilibrator. The equilibrator was perturbed at  $t = -1$  h and air was vented into the equilibrator for about 40 min. The equilibrator was then 'resealed' and the return to equilibrium of CO in the equilibrator was observed in the data record. The data between 0 and 15 h for each of the two experiments was fit by a least squares non-linear fitting routine to a function of the form of Eq. (22).  $C_i$ ,  $\tau_1$ ,  $a$  and  $b$  were found from the fitting routine (Table 4). The equilibration time constant for CO in

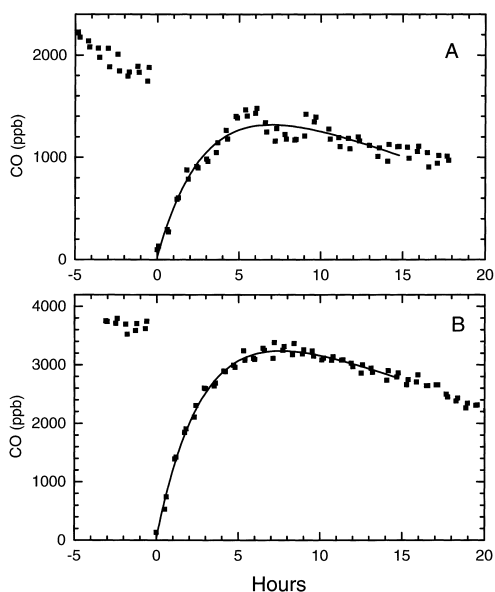


Fig. 6. The CO experiments. In each experiment the CO concentration in the headspace as measured by the GC system is plotted. At 40 min before the zero time the plumbing was reconfigured as shown in Fig. 2(B), and ambient air was drawn into the headspace. The equilibrating plumbing was then reconfigured back to the normal condition (Fig. 2(A)) and the zero time is the time of the first data point after the reconnection. The zero time for (A) was 02:22 local time (LT) on 6 December, the zero time for B was 19:45 on 8 December. The heavy line is a least-squares fit of the data between 0 and 15 h to a function of the form Eq. (21).

the equilibrator for these two experiments was 2.91 and 2.83 h, yielding equilibrator coefficients of 0.37 and 0.38, very close to the values of  $\varepsilon$  for  $\text{CO}_2$  of 0.28 to 0.33.

#### 4.5. Upper water column homogeneity test

The air–sea flux exchange of a trace gas is driven by the difference in the atmospheric and surface water partial pressure. Air–sea exchange studies generally assume that the trace gas concentration at the ship’s water inlet depth of 3–5 m is representative of the surface partial pressure. This assumption can be tested with a detailed profile in the upper few meters of a trace gas that has the potential to have a large vertical concentration gradient. CO is a good tracer for mixing in the upper mixed layer because it is produced photochemically in the upper few meters of the water

Table 4  
Carbon monoxide experiment

|                    | Units  | 6 December | 8 December |
|--------------------|--------|------------|------------|
| Headspace volume   | l      | 19         | 19         |
| Temperature        | °C     | 13.1       | 12.2       |
| Salinity           | PSU    | 34.852     | 34.635     |
| $Q_w$              | l/min  | 13.4       | 13.3       |
| $\alpha$           |        | 0.0227     | 0.0230     |
| $C_i$              | ppb    | 25.73      | 41.06      |
| $A$                | ppb    | 39.32      | 92.28      |
| $B$                | ppb/Hr | −1.34      | −2.34      |
| $\tau$             | Hr     | 2.93       | 2.81       |
| rms fit error, ppb | ppb    | 89         | 72         |
| $\varepsilon$      |        | 0.36       | 0.37       |

$Q_w$  was the measured sample water;  $\alpha$  was the CO solubility [14];  $C_i$ ,  $A$ ,  $B$ , and  $\tau$  were constants calculated from a least squares fit to Eq. (22) of the data shown in Fig. 6;  $\varepsilon$  was determined from the fitted  $\tau$  and Eq. (6).

column and it has a relatively short lifetime (1–6 days) in seawater [13].

A detailed CO profile in the top 5 m was taken under open ocean conditions at 20.5°S, 160°W during the ACE-1/RITS project. Samples were collected mid-day under bright sunlight when the rate of CO production in surface seawater was presumably high. Conditions were relatively calm with wind speeds of 5 m/s and no breaking waves. Samples were collected in duplicate at depths of 0.5, 1, 2, and 5 m depth in hand held, 100 ml glass syringes by scuba divers that were swimming forward at a slow speed. An additional duplicate sample at a depth of 20 cm was collected from a hand held syringe from an operator in the small inflatable boat from which the divers were operating. The samples were stored in the dark and processed on DISCOVERER within 3 h of collection using the CO system described in [13]. This profile (Fig. 7) shows a uniform concentration in the upper 5 m within the expected error range of the measurement ( $\pm 4.7\%$ ). While the cast was being collected, the CO analysis system on DISCOVERER, using a automated purge and trap method, was sampling water collected through the ships seawater sampling system. At the time of the syringe cast, the system on DISCOVERER, located 500 m away, measured a CO concentration of 1.5 nM, 6% lower than the CO concentration of 1.6 nM measured in the syringe sample collected at 2 m depth.

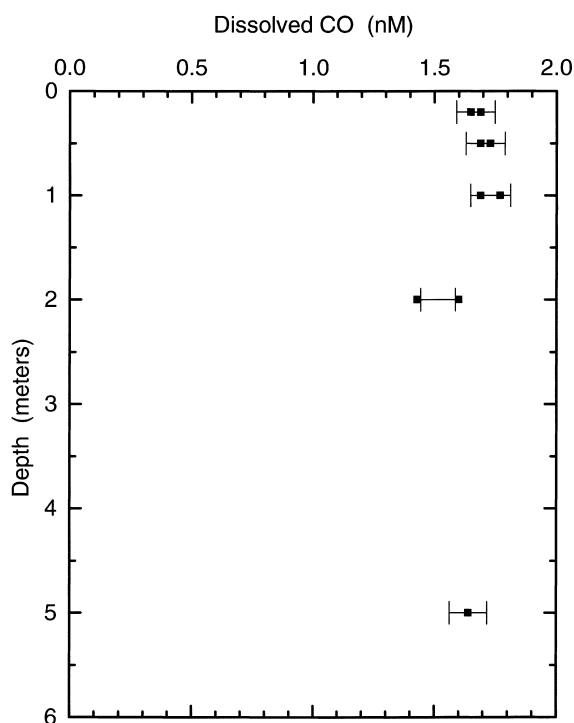


Fig. 7. A depth profile of CO profile in the top 5 m of the open ocean from at 20.5°S, 160°W at 11:50 LT on 28 October, 1995. During the time of sample collection the wind speed was 5 m/s. The samples were collected in 100 ml ground glass syringes by hand with scuba divers. The error bars are the  $\pm 4.7\%$  expected sample error about the mean of the measured values.

## 5. Discussion

We have presented a simple model of a working equilibrator, based on the assumptions of mass con-

tinuity and that the flux of the gas between the sample water stream and equilibrator headspace is a constant fraction,  $\varepsilon$ , of the amount that is thermodynamically able to flux between the equilibrator headspace and the sample water stream. We have provided experimental evidence that  $\varepsilon$  is about 0.3–0.4, both for  $\text{CO}_2$  and CO, two gases with widely differing solubilities. Thus, we believe we can extend our model to make predictions for other gases of known solubility for the deviation from equilibrium due to venting of ambient air into the equilibrator headspace. Table 5 lists the equilibrator time constant ( $\tau_1$ ) for number of trace gases with a range of solubilities predicted with Eq. (6) and for the deviation from equilibrium,  $D$ , as calculated from Eq. (16) for typical, measured vent flow rates of 35 and 80 ml/min. This shows the expected error in the equilibrator for measurements of  $\text{CO}_2$  and  $\text{N}_2\text{O}$  partial pressure is 0.2% or less, is in the range of 2% for less soluble CFCs and  $\text{CH}_4$ , and can be over 25% for CO. The relatively large error expected for CO is due to its low solubility coupled with the large disequilibrium that exists between the surface water and the overlying atmosphere.

The disequilibrium expression Eq. (16) only predicts errors due to venting of ambient air. When errors due to this source are in the part per thousand range, errors due to other process such as lack of precise pressure control in the headspace can be significant. The pressure difference between the equilibrator headspace and the gas measurement cell is important because equilibration is a thermodynamic process and it is the partial pressure of the trace gas in each phase that becomes equal at equilibrium. The accu-

Table 5  
Predictions of the level two model

| Gas                       | $\alpha$ at 25°C | atm | $\tau_1$ (min) | $D$ $Q_v = 35$ | $D$ $Q_v = 80$ |
|---------------------------|------------------|-----|----------------|----------------|----------------|
| $\text{CH}_3\text{CCl}_3$ | 1.35             | 0.1 | 2.9            | 0.0005         | 0.0012         |
| $\text{CO}_2$             | 0.65             | 0.1 | 6.1            | 0.0011         | 0.0025         |
| $\text{N}_2\text{O}$      | 0.62             | 0.1 | 6.4            | 0.0012         | 0.0026         |
| COS                       | 0.37             | 0.5 | 10.7           | 0.0097         | 0.0216         |
| F-11                      | 0.16             | 0.1 | 24.7           | 0.0044         | 0.0094         |
| F-12                      | 0.05             | 0.1 | 79.2           | 0.0127         | 0.0250         |
| $\text{CH}_4$             | 0.025            | 0.1 | 158.3          | 0.0226         | 0.0400         |
| CO                        | 0.0183           | 0.9 | 216.3          | 0.2564         | 0.4290         |

atm is the Eq. (16) pre-existing disequilibrium factor ( $1 - (C_a\alpha/C_w)$ ). The algebraic sign of  $D$  depends on the sign of atm, for these examples it is assumed that atm is positive (sample water supersaturated with respect to the atmosphere), if sample water is undersaturated with respect to the atmosphere then  $D$  will be negative.

racy in any trace gas measurement can only be as good as the ratio of the pressures in the equilibrator headspace and in the trace gas measurement cell. Most users will try to keep both these pressures at ambient atmospheric pressure. However, if one is trying for part per thousand accuracy, the assumption of good pressure control must be checked by careful measurements. Another potential cause of errors in a field measurement system can be biological sources and sinks of the trace gas in the shipboard sampling system. This will be greater for gases of lower solubility and with lower sample water flow rates. One way to minimize these errors is to use a sample water flow that is much greater than that required by the equilibrator, dumping the excess overboard.

An important assumption for this equilibrator model is that any air that is vented into the equilibrator headspace is 'clean' and of known concentration. On a working research ship, engine exhaust and other ship fumes are potential large sources of pollution. If these sources are allowed to vent into the equilibrator, its reliability and state of equilibrium could be greatly compromised. Ideally the vent air should come from upwind of the ship. If this location is of such a distance that unacceptable pressure drops could occur in the equilibrator, then an air pump, (likely already in use for air sample) can be used to draw air down a sample line from a clean location, likely near the ship's bow. The exit from the pump can be directed to the equilibrator vent so long as a vent to the atmosphere is provided near the equilibrator to keep the pressure in the equilibrator headspace at ambient pressure.

One surprising feature of our particular equilibrator is that the vent flow depends on the sample water flow. In particular, as the water flow rate is increased above a flow value of 12 to 18 l/min, the venting flow of air into the equilibrator makes a jump to a much higher value of ~200 ml/min or more. This appears to be due to increased turbulence in the equilibrator causing an increase in air bubbles that are passing through the air lock. Since a low vent flow is critical to the successful operation of an equilibrator, the vent flow rate should be monitored and the water flow rate adjusted to minimize the flow of vent air. A convenient flow meter is an integrating gas meter of the type commonly used to meter natural gas.

## Acknowledgements

I thank T. Bates, R. Feely, P. Murphy, R. Weiss and R. Wanninkhof for comments on the manuscript. The CO<sub>2</sub> measurements were made with the cooperation of R. Feely and C. Costca. This work was carried out under the NOAA Radiatively Important Trace Species (RITS) Program and the Atmospheric Chemistry component of the NOAA Climate and Global Change Program. This is contribution number 1943 from the NOAA Pacific Marine Environmental Laboratory and number 484 from the Joint Institute for the Study of the Atmosphere and Ocean.

## References

- [1] W.S. Broecker, T. Takahashi, *J. Geophys. Res.* 71 (1966) 1575.
- [2] R. Wanninkhof, K. Thoning, *Marine Chem.* 44 (1993) 189.
- [3] J.H. Butler, J.W. Elkins, K.B. Egan, C.M. Brunson, T.M. Thompson, T.J. Conway, Trace gases in and over the west Pacific and east Indian Oceans during the El Niño-Southern Oscillation event of 1987, NOAA Data Rep. ERL ARL-16, Air Resour. Lab., Natl. Oceanic and Atmos. Admin., Boulder, Colo. 1988, 104 pp.
- [4] J.H. Butler, J.W. Elkins, T.M. Thompson, B.D. Hall, *J. Geophys. Res.* 96 (1991) 22347.
- [5] T.S. Bates, K. Kelly, J.E. Johnson, *J. Geophys. Res.* 98 (1993) 16969.
- [6] T.S. Bates, K.C. Kelly, J.E. Johnson, R.H. Gammon, *J. Geophys. Res.* 100 (1995) 23093.
- [7] T.S. Bates, K.C. Kelly, J.E. Johnson, R.H. Gammon, *J. Geophys. Res.* 101 (1996) 6953.
- [8] R.H. Bieri, Dissolved conservative gases in seawater, in: E.D. Goldberg (Ed.), *The Sea*, vol. 5, Wiley, New York, 1974, Chap. 6.
- [9] H. Chen, R. Wanninkhof, R.A. Feely, D. Greeley, Measurement of fugacity of carbon dioxide in sub-surface water: an evaluation of a method based on infrared analysis, NOAA Data Rep. ERL AOML-85, Atlantic Oceanographic and Meteorological Laboratory, Miami, FL, 1995, 152 pp.
- [10] K.S. Johnson, *Limnol. Oceanogr.* 27 (1982) 849.
- [11] R.F. Weiss, *Marine Chem.* 2 (1974) 203.
- [12] R.D. Jones, *Deep Sea Res.* 53 (1995) 341.
- [13] J.E. Johnson, T.S. Bates, *Global Biogeochem. Cycles* 10 (1996) 347.
- [14] D.A. Wiesenburg, N.L. Guinasso Jr., *J. Chem. Eng. Data* 24 (1979) 356.